Crystallization Behavior of Poly(*N*-methyldodecano-12-lactam). IV. Nonisothermal Crystallization

J. Kratochvíl, A. Sikora

Institute of Macromolecular Chemistry, Academy of Sciences of the Czech Republic, 162 06 Prague 6, Czech Republic

Received 18 June 2003; accepted 9 June 2004
DOI 10.1002/app.21255
Published online in Wiley InterScience (www.interscience.wiley.com).

ABSTRACT: Nonisothermal crystallization of poly(*N*-methyldodecano-12-lactam) (MPA) was investigated using DSC method at cooling rates of 2–40 K/min. With increasing cooling rate, crystallization exotherms decreased in magnitude and shifted toward lower temperatures. Subsequent heating runs (10 K/min) showed an exotherm just above T_g, which increased in magnitude with the rate of preceding cooling run, corresponding to the continuation of primary crystallization interrupted as the system crossed T_g on cooling. Kinetic evaluation by the Avrami method gave values of exponent n close to 2.0, suggesting two-dimensional crystal growth combined with heterogeneous nucleation. The Tobin method, covering the intermediate range of relative crystallinities, provided $n \cong 2.20$, suggesting possible partial involvement of homogeneous nucleation at later stages of nonisothermal crystallization. The crystallization rate parameter $k^{1/n}$ showed a linear dependency on cooling rate for both methods, the Tobin values being slightly higher. The Ozawa approach failed to provide reasonable values of the kinetic exponent m of MPA. The Augis–Bennet method was used to determine the effective activation energy of the entire nonisothermal crystallization process of MPA. © 2004 Wiley Periodicals, Inc. J Appl Polym Sci 95: 564–572, 2005

Key words: crystallization; kinetics (polym.); Avrami and Tobin treatment; activation energy; differential scanning calorimetry (DSC)

INTRODUCTION

Poly(*N*-methyldodecano-12-lactam) (MPA) shows a complex crystallization/melting behavior. In the first two parts of our series[1,2] we described three steps taking place during isothermal crystallization and subsequent heating run.

After cooling from the melt to a specific crystallization temperature T_c, a primary lamellar structure is formed, which melts at about 51°C. On subsequent heating during DSC scanning, the same primary crystalline structure is formed by additional crystallization associated with *trans*/*cis* transition on the C—N bond of MPA, the optimum temperature of which was about 30°C. On further heating, the primary structure undergoes recrystallization, associated with arrangement of all-*trans* conformations of CH_2 sequences in the MPA molecules, with the optimum temperature of about 54°C. The final higher-ordered structure melts at about 62°C.

In the third part of our series[3] we studied kinetics of the three steps of the isothermal crystallization process of MPA: (1) primary crystallization from melt at a given T_c, (2) additional crystallization at 30°C, and (3) recrystallization at 54°C.

In the present part of the series, we studied the crystallization of MPA from the melt under nonisothermal conditions. It is generally accepted that, compared with isothermal crystallization, the nonisothermal crystallization process is much closer to real conditions under which polymer processing takes place. During the nonisothermal crystallization process the primary crystalline structure of MPA, with the melting point of about 51°C, is formed. It was our objective to describe the nonisothermal crystallization of MPA from both phenomenological and kinetic perspectives.

The Avrami equation was originally derived to study crystallization kinetics under isothermal conditions.[4,5] Recently, several authors[6–8] successfully applied this approach to study the kinetics of nonisothermal crystallization. The Avrami equation reads:

$$X(t) = 1 - \exp(-kt^n) \quad (1)$$

where $X(t)$ is the relative crystallinity at time t; n is the Avrami exponent related to nucleation type and dimensionality of crystal growth; and k is the kinetic constant, which is a function of nucleation density and rate of crystal growth.

It should be noted that the kinetic parameters n and k derived from eq. (1) under nonisothermal conditions do not have the same meaning as corresponding parameters obtained from isothermal measurements.

Correspondence to: J. Kratochvíl (jakr@imc.cas.cz).
Contract grant sponsor: Grant Agency of the Academy of Sciences of the Czech Republic; contract grant number: A4050007.

They are rather used as two adjustable parameters in fitting the data obtained on cooling at constant rate to eq. (1) and comparing the kinetics of the process under different cooling rates.

It is well known that the Avrami approach was derived and can be used only for early stages of the crystallization process. Tobin[9] took into consideration the effect of the growth site impingement and arrived at an equation that could describe the crystallization process up to relative crystallinities of 50%. The Tobin equation reads:

$$\frac{X}{1-X} = kt^n \tag{2}$$

where the symbols have a meaning similar to those of the Avrami eq. (1). Recently, some authors[8,10] successfully applied the Tobin approach to study kinetics of nonisothermal crystallization at higher relative crystallinities.

Ozawa[11] extended the Avrami approach to nonisothermal conditions by assuming that the nonisothermal crystallization process running at constant cooling rate could be approximated by a series of infinitesimal isothermal steps and that no secondary crystallization took place. He came to the following equation:

$$X = 1 - \exp\left(\frac{-K(T)}{\Phi^m}\right) \tag{3}$$

where X is the relative crystallinity, Φ is the cooling rate, $K(T)$ is a complex cooling function that constitutes nucleation density and crystal growth rate, and m is an exponent that reflects dimensionality of crystal growth.

Several equations have been proposed for determining the effective activation energy from the nonisothermal crystallization data.[8] The approach of Augis and Bennet[12] was identified to be most theoretically correct. In the Augis–Bennet equation

$$d\left(\ln\frac{\Phi}{T_0 - T_p}\right) = -\frac{\Delta E}{R}\, d\left(\frac{1}{T_p}\right) \tag{4}$$

where Φ is the cooling rate, T_p is the temperature of the minimum of the DSC exotherm, T_0 is a standard temperature in the melt, and R is the gas constant. This equation does not imply any particular model and was recently successfully applied to determine the effective activation energy of the entire crystallization process in polymer systems.[8]

EXPERIMENTAL

The measurements were carried out with three samples of MPA. Their denotation, MPA 5, MPA 15, and MPA 45, corresponds to their approximate weight-average molecular weights 5000, 15,000 and 45,000, respectively. For details, the reader is referred to the first part of this series.[1]

A Perkin–Elmer Pyris 1 DSC apparatus (Perkin Elmer Cetus Instruments, Norwalk, CT) was used for calorimetric measurements. The samples of about 10 mg were sealed in aluminum pans, and the system was cooled with liquid nitrogen and flushed with helium. Indium and cyclohexane were used to calibrate the temperature scale.

The samples were first quickly heated to 90°C, and held at this temperature for 10 min to remove all residual crystalline structure. The cooling scans were made at the rates 2, 5, 10, 20 and 40 K/min, and the final cooling temperature was −50°C. Subsequent heating runs were performed at the rate 10 K/min in all cases.

When comparing results obtained at different cooling rates, it is necessary to correct the temperature scale for the lag between temperature of the polymer and that of the sample holder. In the literature, this problem is addressed in various ways ranging from a purely empirical correction[13] to application of quite complex equations of heat transfer.[14,15] In our study we have adopted a compromise approach recently suggested by Martins and Cruz Pinto,[10] which is based on the fact that some liquid-crystalline compounds show quite fast transitions between respective structures and can thus be used for calibrating the temperature scale of DSC instruments. We used 4,4′-azoxyanisole (AZA), which shows a nematic/isotropic (N/I) transition at about 134°C.

The temperatures of the N/I transition of AZA measured in the range of cooling/heating rates from −80 to +80 K/min show a smooth, symmetrical, slightly curved dependency, which crosses the axis of zero rate at 134.1°C. The difference between this value and the temperature of the N/I transition of AZA measured at respective cooling rates was used as a positive correction of the temperature scale. At the cooling rate 40 K/min, this correction amounted to +1.80°C.

It should be noted, however, that this compromise approach is based on the assumption that a liquid-crystalline substance shows approximately the same thermal resistance as that of the melted polymer in the sample pan. Throughout this study, in all cases when comparison is made of results obtained at different cooling rates, the temperature scale was corrected by the above-described procedure.

RESULTS AND DISCUSSION

Evaluation of exotherms

The exotherms of MPA 5 scanned on cooling at different cooling rates are shown in Figure 1. The respective curves were corrected for difference in the DSC signal attributed to different cooling rates. Some typ-

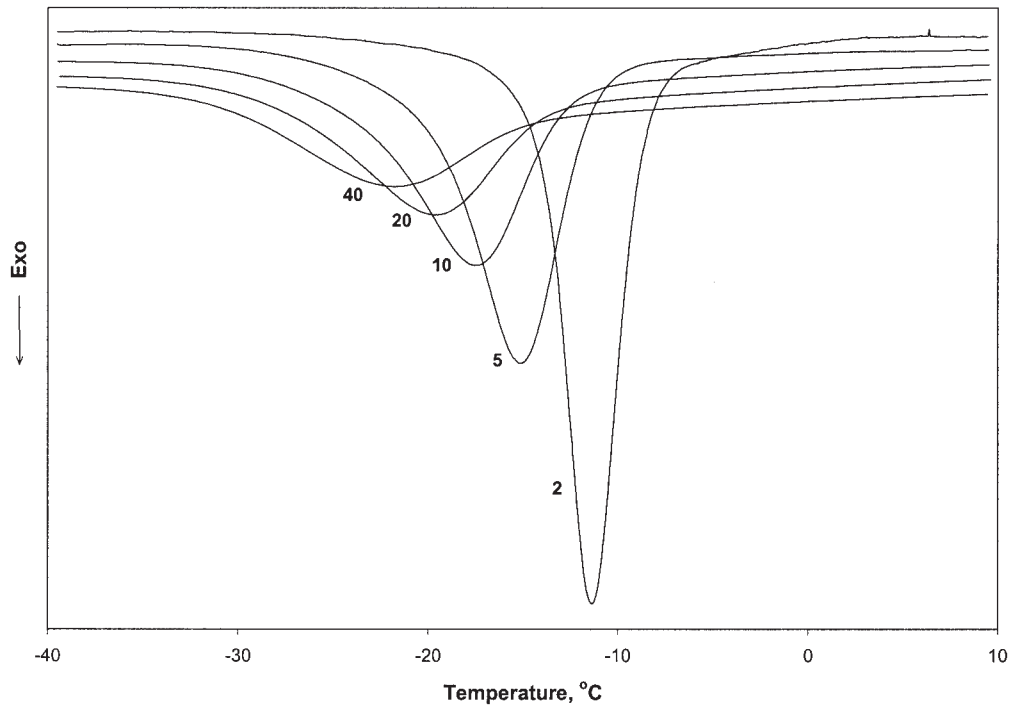

Figure 1 Crystallization exotherms of MPA 5 obtained on cooling from melt at indicated cooling rates (K/min).

ical features can be deduced from the figure. The overall area of the exotherms, that is, crystallization enthalpy ΔH_c, decreases with increasing cooling rate. An approximately linear decrease in ΔH_c with logarithm of cooling rate is shown in Figure 2. The peak temperature T_p, that is, the point of maximum crystallization rate, shifts toward lower temperatures with increasing cooling rate. This fact is documented in Figure 3 where, in addition to T_p, a linear dependency of the reciprocal time of the exotherm minimum $1/t_p$ on cooling rate is also shown.

The dependencies of T_p on cooling rate in Figure 3 can be extrapolated (by fitting a polynomial of the 3rd order) to $\Phi = 0$ K/min to obtain an "equilibrium crystallization temperature." In the literature this parameter is interpreted as an ultimate temperature at which crystallization of a polymer system can be achieved on cooling from the melt.[16] The approximate values of this temperature are +0.5, −7.0, and −10.0°C for MPA 5, MPA 15, and MPA 45, respectively.

The thermograms of heating runs of MPA 5, scanned after nonisothermal crystallization at respective cooling rates, are shown in Figure 4. In this case, the heating rate was the same, 10 K/min, in all cases. Thus, the differences between respective curves are to be attributed to the preceding cooling runs at different cooling rates only.

The traces in Figure 4 show some typical features of the complex crystallization/melting behavior of MPA, as discussed in the first two parts of our series.[1,2] After passing the glass-transition temperature T_g at about

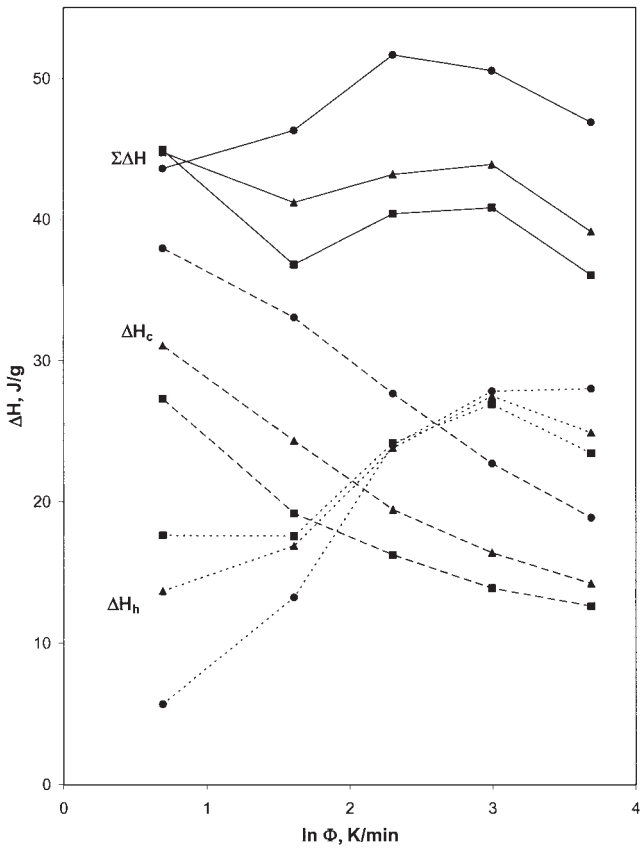

Figure 2 Dependencies of heats of crystallization on logarithm of cooling rate: ΔH_c on cooling (dashed lines), ΔH_h on subsequent heating (dotted lines), $\Sigma\,\Delta H = \Delta H_c + \Delta H_h$ (solid lines); MPA 5 (circles), MPA 15 (triangles), MPA 45 (squares).

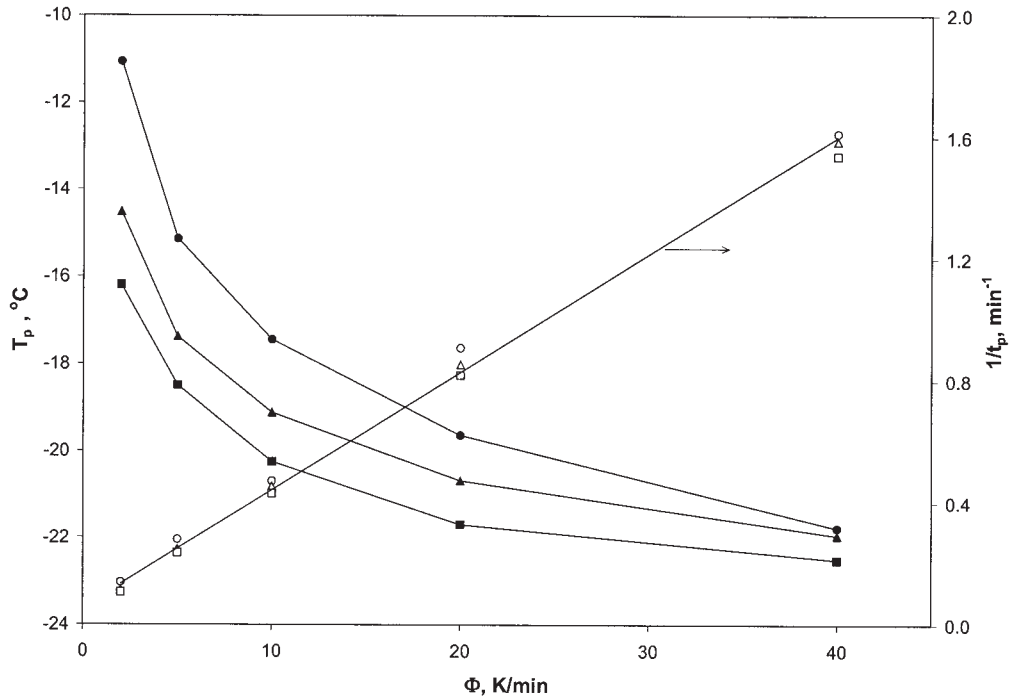

Figure 3 Dependency of exotherm peak temperature T_p (solid symbols) and reciprocal time of exotherm peak $1/t_p$ (open symbols) on cooling rate: MPA 5 (circles), MPA 15 (triangles), MPA 45 (squares).

−30°C, the curves show the first exotherm, the minimum of which shifts from 0 to −15°C as the rate of the previous cooling run increases. The second deep exotherm, with the minimum at about 30°C, is associated with additional crystallization of MPA.[1,3] The primary crystalline structure formed during the preceding crystallization stages melts at about 51°C. This melting endotherm is followed by a recrystallization exotherm with a minimum at about 54°C. The final higher-ordered structure formed by recrystallization melts at about 62°C.

The main difference between the respective thermograms in Figure 4 is associated with the first exotherm appearing just after T_g. The area of this exotherm, and thus the heat ΔH_h liberated during the crystallization process taking place after the system crosses T_g on heating, increases with the value of Φ of the preceding nonisothermal cooling run. This trend goes in parallel with an opposite trend of crystallization enthalpies on cooling ΔH_c (see Fig. 1). Both dependencies are shown in Figure 2 together with their sums $\Sigma\,\Delta H = \Delta H_c + \Delta H_h$. The error in determining these quantities was estimated at ±1–2%, in line with generally accepted accuracy of DSC measurements.[17] Obviously, the crystallization process taking place during cooling at different Φ values and interrupted as the system is cooled below T_g continues on subsequent heating.

It should be noted, however, that the values of ΔH_h and thus $\Sigma\,\Delta H$ can be considered semiquantitative only. This is because the values of ΔH_h cannot be unambiguously determined, given that the DSC

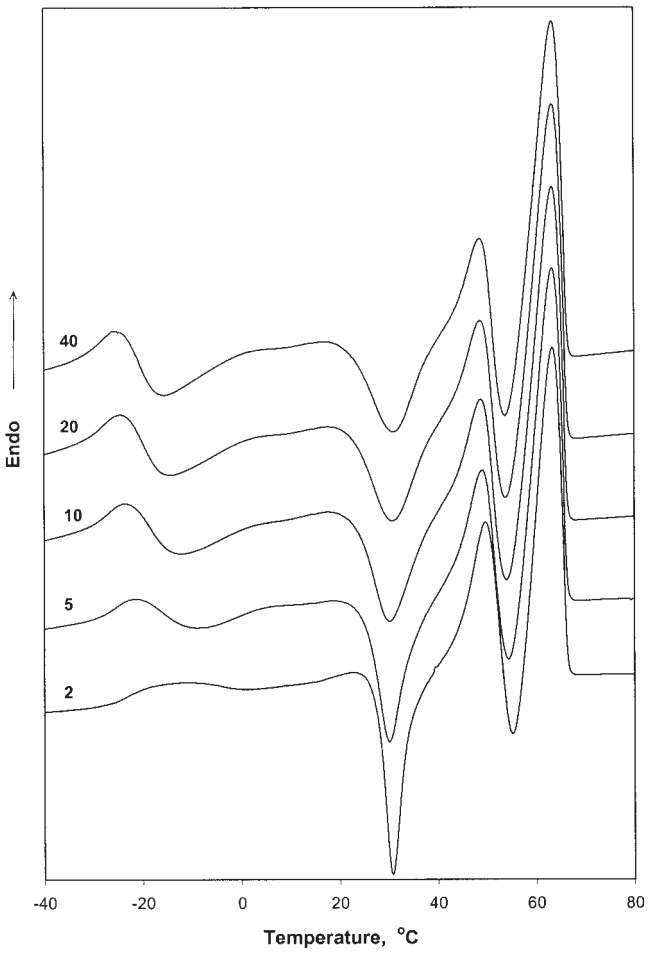

Figure 4 Heating runs (10 K/min) of MPA 5 after crystallization on cooling at indicated cooling rates (K/min).

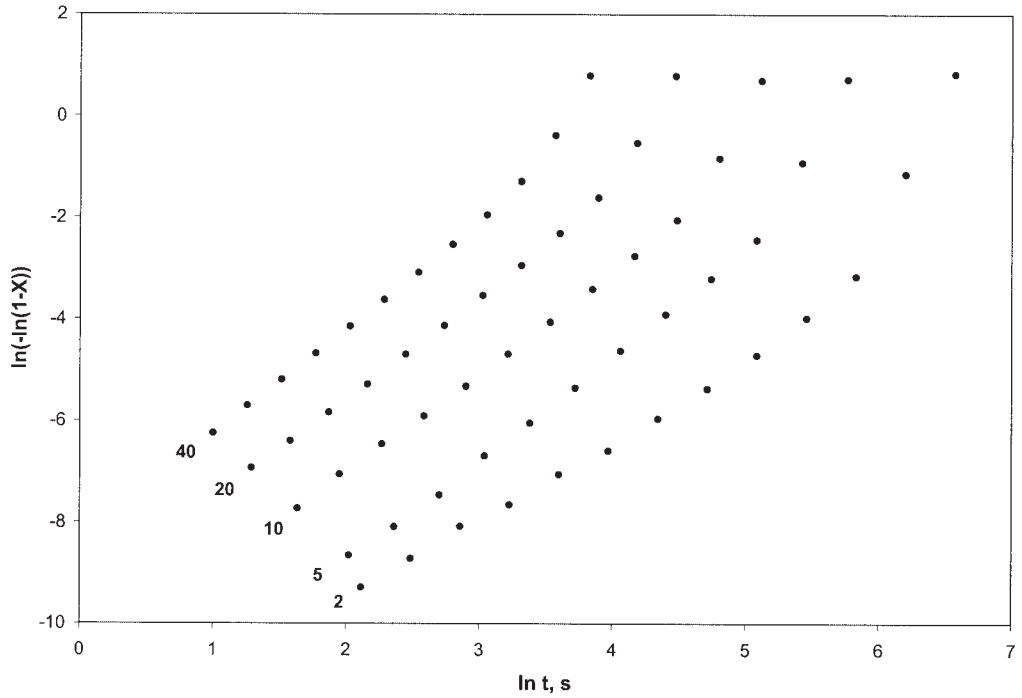

Figure 5 Avrami plots of nonisothermal crystallization of MPA 15 at indicated cooling rates (K/min).

traces in Figure 4 reflect the net product of all parallel and/or consecutive thermal processes taking place during heating the MPA sample. In this case, in particular, these are crystallization after passing T_g and beginning of additional crystallization associated with the exotherm at +30°C. Finally, we can state that the primary crystalline structure of MPA melting at about 51°C is formed in three subsequent steps: (1) nonisothermal crystallization on cooling, (2) crystallization after the system passes T_g on heating, and (3) additional crystallization with an optimum at +30°C.

Avrami approach

The values of relative crystallinity obtained by stepwise integration of nonisothermal crystallization exotherms were first processed using the Avrami approach with eq. (1). The resulting Avrami plots of MPA 15 for different cooling rates are shown in Figure 5. Major initial parts of these plots have a linear character, which allows the kinetic parameters to be determined. The results of Avrami evaluation are summarized in Table I. The ranges of linearity of the plots in Figure 5 taken into the kinetic evaluation are shown in the columns denoted X_{lin} in Table I. Thus, the range of relative crystallinity of 0.01 to about 15% reflects applicability of the Avrami approach to nonisothermal crystallization kinetics.

The values of exponent n of all three samples of MPA closely oscillate around 2.0, without any significant dependency on either cooling rate or molecular weight. The average values of 2.01 to 2.05 are in substantial agreement with the results of our studies[3] on kinetics of isothermal crystallization of MPA and support the idea of a two-dimensional crystal growth combined with heterogeneous nucleation at lower supercoolings, that is, at higher temperature of isothermal crystallization and at initial stages of nonisothermal crystallization.

TABLE I
Nonisothermal Crystallization Kinetic Parameters of MPA Derived from Avrami Equation

ϕ (K/min)	MPA 5			MPA 15			MPA 45		
	X_{lin} (%)	n	ln k	X_{lin} (%)	n	ln k	X_{lin} (%)	n	ln k
2	0.01–3.2	1.95	−14.05	0.01–1.9	1.84	−13.50	0.01–2.7	1.78	−13.05
5	0.02–4.3	2.15	−14.42	0.02–4.0	2.03	−12.80	0.02–4.6	2.08	−13.05
10	0.03–5.9	2.03	−11.90	0.04–6.2	2.05	−11.10	0.05–6.4	2.06	−11.25
20	0.08–8.1	2.04	−10.10	0.10–9.5	2.03	−9.50	0.12–10.3	2.05	−9.60
40	0.14–9.7	2.06	−8.65	0.19–13.3	2.12	−8.40	0.22–14.6	2.06	−8.25
	Average 2.05			Average 2.01			Average 2.01		

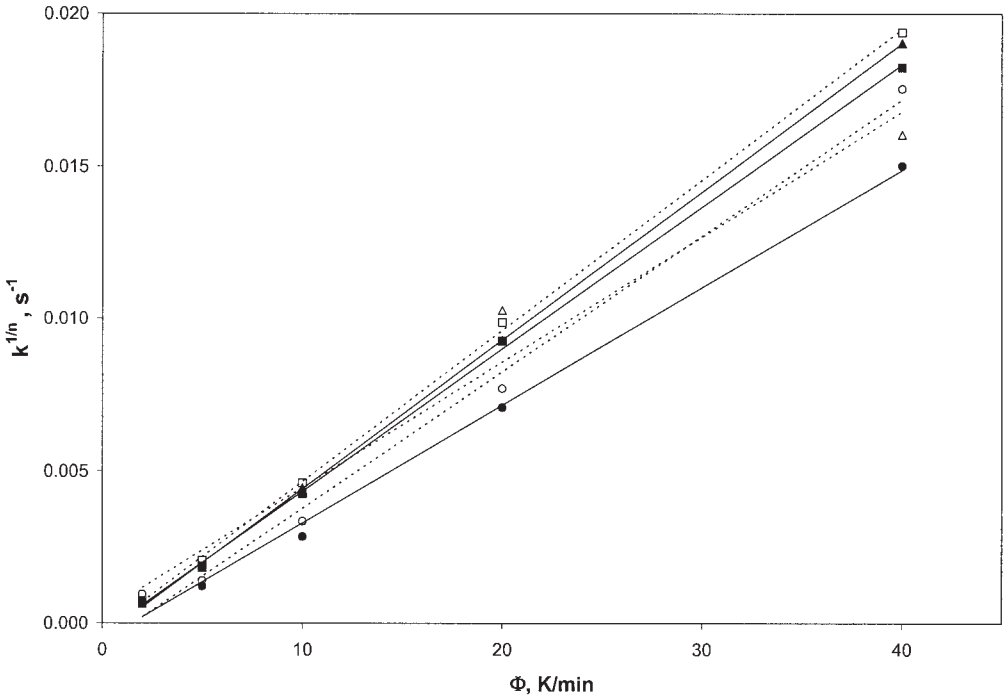

Figure 6 Dependency of crystallization rate parameter on cooling rate: Avrami method (solid symbols, solid lines), Tobin method (open symbols, dotted lines); MPA 5 (circles), MPA 15 (triangles), MPA 45 (squares).

The values of kinetic constant k increase, as expected, with cooling rate. Here, the fact is reflected that, with increasing cooling rate, the system has less time to complete crystallization and, therefore, it reaches lower degrees of absolute crystallinity. The crystallization rate parameter[6,15] $K = k^{1/n}$ shows a linear dependency on cooling rate, as shown in Figure 6.

Tobin approach

An alternative approach to evaluating kinetic parameters was proposed by Tobin[9] who took into consideration the effect of the growth site impingement and suggested that eq. (2) could be applied to relative crystallinities up to 50%. Some authors successfully used this method to process nonisothermal crystallization data.[8,10] The Tobin plots obtained using eq. (2) for different cooling rates are shown in Figure 7. The plots have a character similar to that of the Avrami approach in Figure 5. However, the range of linearity and, thus, applicability of the Tobin approach covers relative crystallinities of about 0.05–44%, as shown in the columns denoted X_{lin} in Table II.

The values of Tobin exponent n listed in Table II are generally somewhat higher than those of the Avrami approach in Table I. Noninteger values of the kinetic exponent in crystallizing polymer systems are quite often discussed in the literature and interpreted as various combinations of nucleation/growth mechanisms.

From the average values of n = 2.12–2.22 we might speculate that at later stages of nonisothermal crystallization covered by the Tobin treatment, that is, under higher supercoolings, heterogeneous nucleation suggested above on the basis of the Avrami equation might be accompanied by a homogeneous mechanism leading to increased values of n. Similar trends were revealed in our studies[3] on isothermal crystallization of MPA, where the value of the Avrami exponent n increases from approximately 2.0 to 2.5 with increasing supercooling. These findings, however, should be supported by independent (such as microscopic) studies.

Similarly to the above-discussed Avrami approach, the values of ln k in Table II increase sharply with rising cooling rate. The values of the crystallization rate parameter $k^{1/n}$ show linear dependencies on cooling rate (Fig. 6). Generally, the values of $k^{1/n}$ obtained from the Tobin equation are somewhat higher than those from the Avrami method, which could reflect the fact that the Tobin approach covers the region of intermediate conversions where the nonisothermal crystallization of MPA proceeds with the rate close to its maximum.

Ozawa approach

The Ozawa model[11] for evaluating nonisothermal kinetic parameters is frequently applied to polymer systems.[8,18] However, quite often this approach failed to adequately describe the nonisothermal crystallization process.[6,7] The problem is usually ascribed to the fact that the values of relative crystallinity for various cooling rates at a given temperature, necessary for the

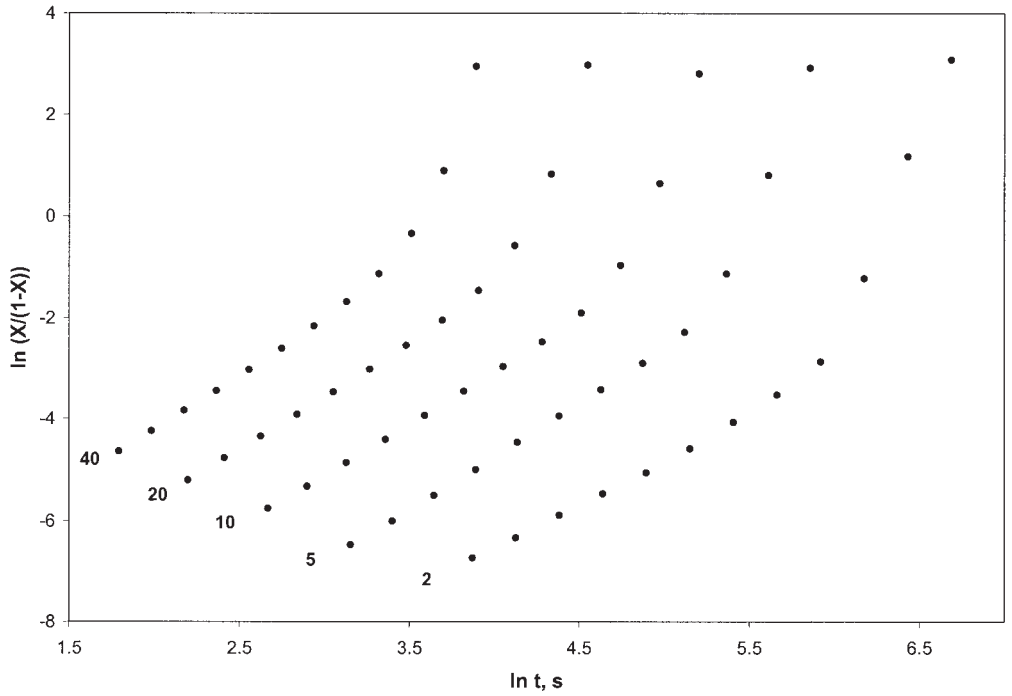

Figure 7 Tobin plots of nonisothermal crystallization of MPA 15 at indicated cooling rates (K/min).

Ozawa evaluation, correspond to different stages of the nonisothermal crystallization process.

The Ozawa plots of MPA 5 obtained from the crystallization exotherms using eq. (3) are shown in Figure 8. The plots are, at least approximately, linear in the temperature range of −32 to −16°C only. However, the values of exponent m evaluated from the slopes of these linear plots vary in the range 0.28 to 1.1, 0.20 to 0.77, and 0.14 to 0.37 for MPA 5, MPA 15, and MPA 45, respectively. It is obvious from these figures that, although the Ozawa approach gives linear plots in at least a limited temperature range when applied to the MPA data, it fails to provide physically reasonable values of the kinetic exponent m.

The reason could partially be associated with the fact that one of the Ozawa presumptions—absence of secondary crystallization—is not fulfilled in the case of MPA, as shown in the first part of our series.[1] Therefore, no attempts have been made at evaluating the cooling rate function $K(T)$ from our data using eq. (3).

Activation energy

Several approaches to access activation energy of the nonisothermal crystallization process in polymer systems have been discussed in the literature.[8] The most frequently used is the Kissinger approach.[19] On the other hand, eq. (4) of Augis and Bennet was found to be most theoretically correct.[8] This allows the effective activation energy of the whole nonisothermal crystallization process to be determined from parameters of the cooling exotherms only, that is, without using any particular kinetic model.

The approach of Augis and Bennet[12] requires a standard temperature in the melt T_0 to be specified for the given polymer system. We have chosen $T_0 = +90$°C, that is, the starting temperature of melted MPA in the cooling process at respective constant cooling rates. As a matter of fact, the results of the Augis–Bennet treatment of nonisothermal crystallization of MPA were found to be scarcely sensitive to the value of T_0 chosen

TABLE II
Nonisothermal Crystallization Kinetic Parameters of MPA Derived from Tobin Equation

ϕ (K/min)	MPA 5			MPA 15			MPA 45		
	X_{lin} (%)	n	ln k	X_{lin} (%)	n	ln k	X_{lin} (%)	n	ln k
2	0.07–22.8	2.18	−15.15	0.12–22.7	2.05	−14.90	0.15–23.6	1.98	−14.29
5	0.04–25.7	2.24	−14.72	0.15–24.4	2.15	−13.30	0.14–26.0	2.16	−13.36
10	0.14–26.8	2.22	−12.65	0.32–27.6	2.13	−11.59	0.30–28.2	2.19	−11.78
20	0.33–33.2	2.18	−10.61	0.55–36.0	2.21	−10.12	0.58–36.7	2.15	−9.93
40	0.67–35.2	2.26	−9.14	0.96–41.6	2.17	−8.97	1.13–43.7	2.12	−8.36
	Average 2.22			Average 2.14			Average 2.12		

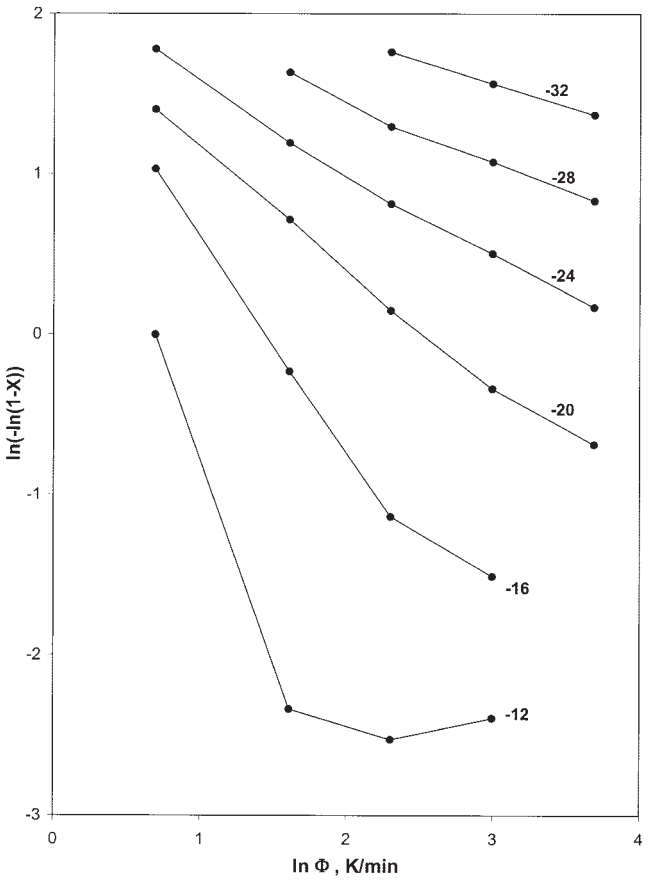

Figure 8 Ozawa plots of MPA 5 at indicated temperatures (°C).

within the range between 65°C (the approximate equilibrium melting temperature of MPA) and 90°C.

The Augis–Bennet plots of the three MPA samples are shown in Figure 9. The least-squares fits of these data give the values of −149, −211, and −240 kJ/mol for the effective activation energy of the whole nonisothermal crystallization process of MPA 5, MPA 15, and MPA 45, respectively.

CONCLUSIONS

Nonisothermal crystallization of MPA was studied at cooling rates between 2 and 40 K/min using the DSC method. The temperature scales at different cooling rates were corrected by means of the data on the N/I transition of 4,4′-azoxyanisole.

With increasing cooling rate the crystallization exotherms shift to lower temperatures and the total crystallinity of MPA decreases. The reciprocal time of crystallization peak shows a linear dependency on cooling rate. The plots of exotherm peak temperature versus cooling rate provide approximate values of the "extrapolated crystallization temperature" +0.5, −7.0, and −10.0°C for MPA 5, MPA 15, and MPA 45, respectively. This parameter is usually interpreted as an ultimate temperature at which crystallization of a polymer system from the melt can be achieved under nonisothermal conditions.

The exotherm appearing on DSC heating scans just after the system passes T_g increases in its magnitude with cooling rate of the preceding cooling run and corresponds to continuation of the crystallization process, interrupted when the system was cooled below T_g during cooling. The primary crystalline structure of MPA melting at about 51°C is formed in three subsequent steps: nonisothermal crystallization at a given cooling rate, crystallization after the system crosses T_g on heating, and additional crystallization with the optimum at about +30°C.

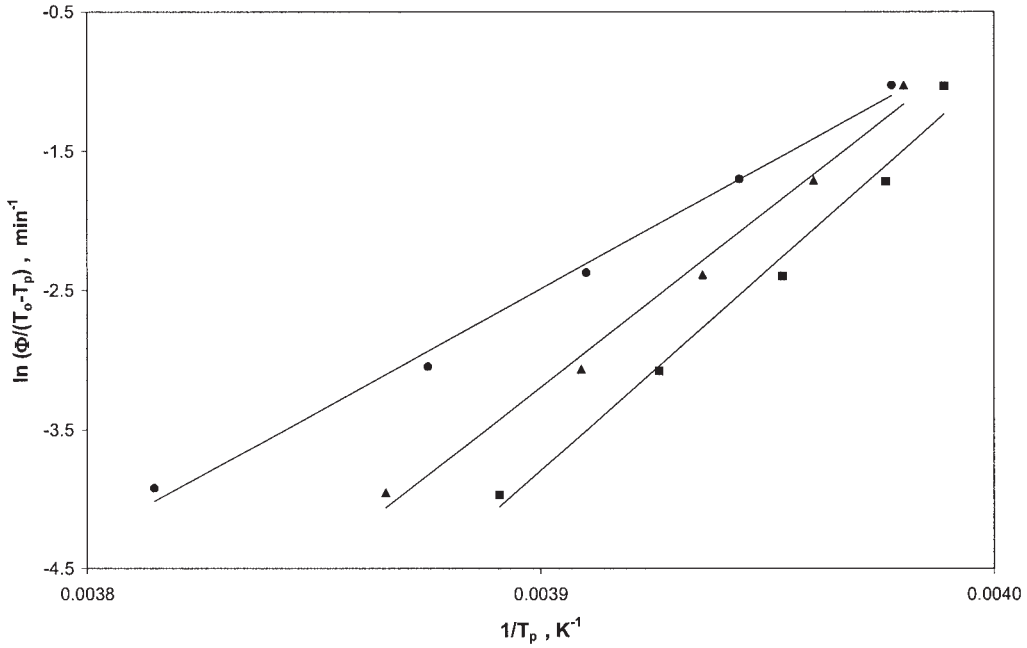

Figure 9 Augis–Bennet plots of MPA 5 (circles), MPA 15 (triangles), and MPA 45 (squares).

The Avrami, Tobin, and Ozawa approaches were adopted for evaluating kinetic parameters of nonisothermal crystallization of MPA. The Avrami evaluation, covering the range of relative crystallinities about 0.01–15%, provides the kinetic exponent $n \cong 2.0$ independent of cooling rate or molecular weight. This suggests a two-dimensional crystal growth combined with heterogeneous nucleation. The Tobin approach, covering the range of relative crystallinity up to about 44%, provides the values of $n \cong 2.2$. This might suggest a partial involvement of homogeneous nucleation at later stages of nonisothermal crystallization. Both these facts comply with our results on isothermal crystallization of MPA.

The kinetic constants k evaluated by the Avrami and Tobin methods increase with cooling rate. The crystallization rate parameter $k^{1/n}$ shows a linear dependency on cooling rate. The data obtained from the Tobin method are generally somewhat higher than those from the Avrami approach, which might reflect the fact that in the region of intermediate conversions covered by the Tobin approach the nonisothermal crystallization of MPA proceeds at a rate close to its maximum.

The Ozawa method, although giving linear plots in a limited temperature region, failed to provide physically reasonable values of the kinetic exponent for nonisothermal crystallization of MPA.

The Augis–Bennet approach has been applied to determining the effective activation energy of the whole nonisothermal crystallization process. The values −149, −211, and −240 kJ/mol were obtained for MPA 5, MPA 15, and MPA 45, respectively.

The authors thank the Grant Agency of the Academy of Sciences of the Czech Republic (Grant A4050007) for financial support.

References

1. Kratochvíl, J.; Sikora, A.; Baldrian, J.; Dybal, J.; Puffr, R. Polymer 2000, 41, 7653.
2. Kratochvíl, J.; Sikora, A.; Baldrian, J.; Dybal, J.; Puffr, R. Polymer 2000, 41, 7667.
3. Kratochvíl, J.; Sikora, A. J Appl Polym Sci 2004, 93, 279.
4. Avrami, M. J Chem Phys 1939, 7, 1103; 1940, 8, 212.
5. Mandelkern, L.; Quinn, F. A.; Flory, P. J. J Appl Phys 1954, 25, 830.
6. Srinivas, S.; Babu, J. R.; Riffle, J. S.; Wilkes, G. L. Polym Eng Sci 1997, 37, 497.
7. Liu, S. L.; Chung, T. S. Polymer 2000, 41, 2781.
8. Supaphol, P. J Appl Polym Sci 2000, 78, 338.
9. Tobin, M. C. J Polym Sci Polym Phys Ed 1974, 12, 399; 1976, 14, 2253.
10. Martins, J. A.; Cruz Pinto, J. J. C. J Macromol Sci Phys B 2000, 39, 711.
11. Ozawa, T. Polymer 1971, 12, 150.
12. Augis, J. A.; Bennet, J. E. J Therm Anal 1978, 13, 283.
13. Mubarak, Y.; Harkin-Jones, E. M. A.; Martin, P. J.; Ahmad, M. Polymer 2001, 42, 3171.
14. Janeschitz-Kriegl, H.; Wippel, H.; Paulik, C.; Eder, G. Colloid Polym Sci 1993, 271, 1107.
15. Sajkiewicz, P.; Carpaneto, L.; Wasiak, A. Polymer 2001, 2, 5365.
16. Papageorgiou, G. Z.; Karayannidis, G. P. Polymer 2001, 44, 2637.
17. Richardson, M. J.; Charsley, E. L. In: Handbook of Thermal Analysis and Calorimetry; Brown, M. E., Ed.; Elsevier: Amsterdam, 1998; Vol. 1, p. 547.
18. Lee, S. W.; Cakmak, M. J Macromol Sci Phys B 1998, 37, 501.
19. Kissinger, H. E. J Res Natl Bur Stand 1956, 57, 217.